LA-UR- 09-01007

Approved for public release;
distribution is unlimited.

Title:	Analysis of Godiva-IV Delayed-Critical and Static Super-Prompt-Critical Conditions
Author(s):	Russell D. Mosteller Joetta M. Goda
Intended for:	2009 International Conference on Advances in Mathematics, Computations, and Reactor Physics Saratoga Springs, NY May 3 - 7, 2009

Form 836 (7/06)

International Conference on Mathematics, Computational Methods & Reactor Physics (M&C 2009)
Saratoga Springs, New York, May 3-7, 2009, on CD-ROM, American Nuclear Society, LaGrange Park, IL (2009)

ANALYSIS OF GODIVA-IV DELAYED-CRITICAL AND SUPER-PROMPT-CRITICAL CONDITIONS

Russell D. Mosteller and Joetta M. Goda
Los Alamos National Laboratory
Los Alamos, NM, USA 87545
mosteller@lanl.gov; jgoda@lanl.gov

ABSTRACT

Super-prompt-critical burst experiments were conducted on the Godiva-IV assembly at Los Alamos National Laboratory from the 1960s through 2005. Detailed and simplified benchmark models have been constructed for four delayed-critical experiments and for the static phase of a super-prompt-critical burst experiment. In addition, a two-dimensional cylindrical model has been developed for the super-prompt-critical condition. Criticality calculations have been performed for all of those models with four modern nuclear data libraries: ENDF/B-VI, ENDF/B-VII.0, JEFF-3.1, and JENDL-3.3. Overall, JENDL-3.3 produces the best agreement with the reference values for k_{eff}.

Key Words: Godiva-IV, benchmark, nuclear data, MCNP

1. INTRODUCTION

Super-prompt-critical burst experiments were conducted on the Godiva-IV assembly at the Los Alamos Critical Experiments Facility at Los Alamos National Laboratory from the 1960s through 2005. Conduct of delayed-critical experiments prior to the prompt burst experiment itself was an essential part of the process. Furthermore, at the start of the burst experiment, the assembly typically remained at room temperature in a static super-prompt-critical condition for a short time, because the only source of neutrons in the assembly was spontaneous fission, and several seconds often elapsed before a self-sustaining chain reaction began. The five experiments discussed herein were performed on April 11, 2003. Detailed and simplified benchmark models have been developed for four delayed-critical configurations and for the static super-prompt-critical portion of the burst experiment. In addition, a two-dimensional cylindrical model has been developed for the static super-prompt-critical condition.

2. DESCRIPTION OF GODIVA-VI

Unlike the core in the initial Godiva experiment [1,2], the Godiva-IV core was basically cylindrical rather than spherical. In addition, it had a hollow glory hole in its center and structural restraints to keep it intact during a prompt-burst experiment. During such

experiments, the excursion was terminated by thermal expansion of the core. Thermal expansion also caused the bottom central part of the core known as the safety block to disengage from the electromagnet that held it in place and drop out of the core, ensuring that the assembly remained subcritical thereafter.

The core of the Godiva-IV assembly contained six stacked rings, an inner subassembly plate with two components, a central spindle, an alignment pin, a shim ring, two control rods, a burst rod, the safety block, and a base for the safety block. Two thermocouples to measure the temperature rise during the excursion also were present. The stacked rings enclosed the inner subassembly plate, the safety block, and the safety-block base. Hollow cylinders within the rings permitted passage of the control and safety rods, which were in symmetric locations, 120° apart. The rings, the inner subassembly plate, the control rods, the burst rod, and the safety block all were made from an alloy of highly enriched uranium (HEU) and molybdenum. The spindle, the alignment pins, the shim ring, and the base for the safety block were made from various types of steel.

Since the control and burst rods contained mostly HEU, they increased reactivity as they were inserted and reduced reactivity as they were withdrawn. When the assembly was not in operation, the safety block and its base were withdrawn to a position such that the top of the safety block was only slightly higher than the bottom of the mounting plate of the assembly machine, and the control and burst rods were fully withdrawn. However, even when the control and burst rods were fully withdrawn, the tops of those rods still were inside the bottom fuel ring.

Restraints for the core included three clamps, three clamp supports, a circular belly band, a subassembly cover plate, a loading ring, three support pads, and several nuts and bolts. The restraints were made from various types of steel. The loading ring fitted into the top of the top fuel ring, and the support pads fitted into the bottom of the bottom fuel ring. The subassembly cover plate sat above the inner subassembly plate, inside the loading ring and enclosing a section of the spindle. Each clamp had top and bottom prongs that fitted onto the top of the loading ring and the bottom of one of the support pads, respectively. The central portion of each clamp fitted into notches in the outer edges of the fuel rings. Each of the three clamps fitted into a slot in its clamp support and was bolted to it. The tops of the clamp supports were held in place by the belly band, and the bottoms of the clamp supports were bolted to the mounting plate. Figures 1 and 2 provide top and side views, respectively, of the Godiva-IV core and its restraints, and a schematic of the core and its restraints is presented in Figure 3. Restraints and core components that were made from the same type of steel appear in the same color in Figure 3.

The core and its restraints were enclosed inside a thin cylindrical core cover that was made of aluminum. Similarly, a contamination shield made of steel and plastic was attached to the bottom of the mounting plate, enclosing the safety block and the bottoms of the control rods and the burst rod when they were withdrawn.

The four delayed-critical configurations and the static super-prompt-critical configuration discussed herein differed only in the positions of the two control rods and the burst rod. A summary of the positions of those rods is presented in Table I. The full stroke of the burst rod

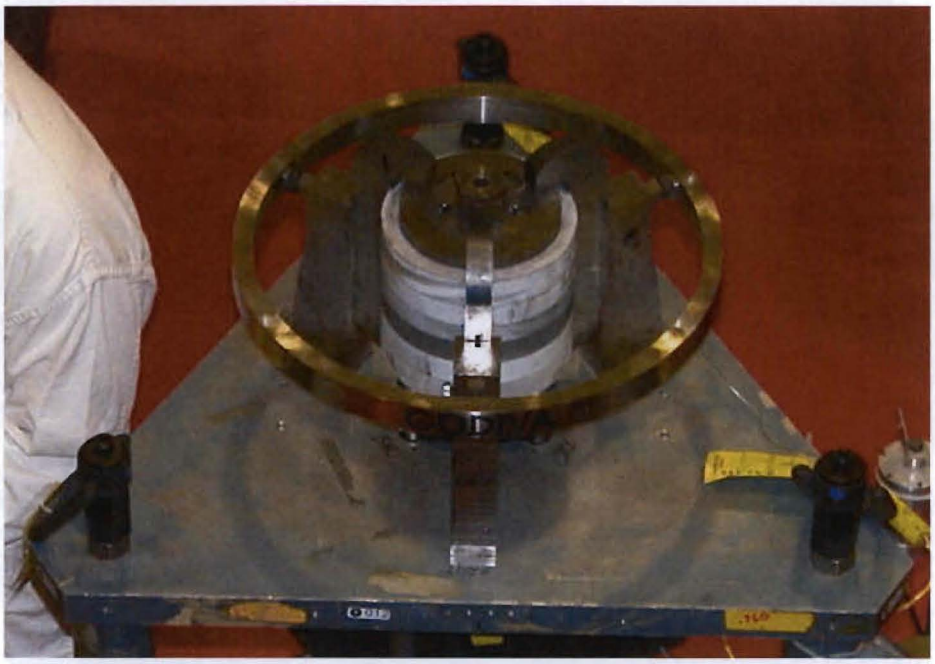

Figure 1. Top view of the Godiva-IV assembly.

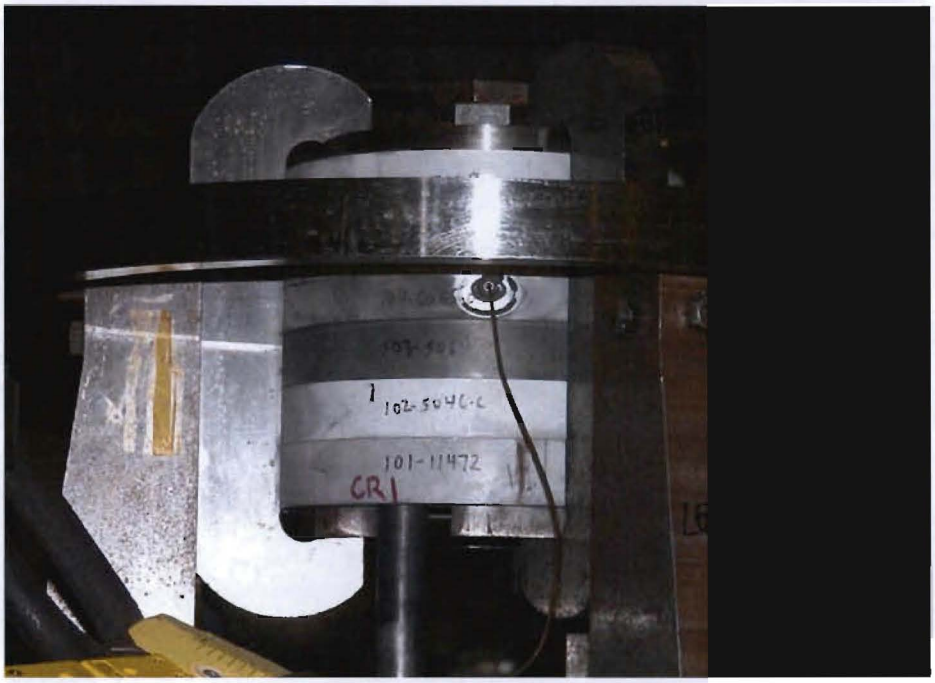

Figure 2. Side view of the Godiva-IV core and its restraints.

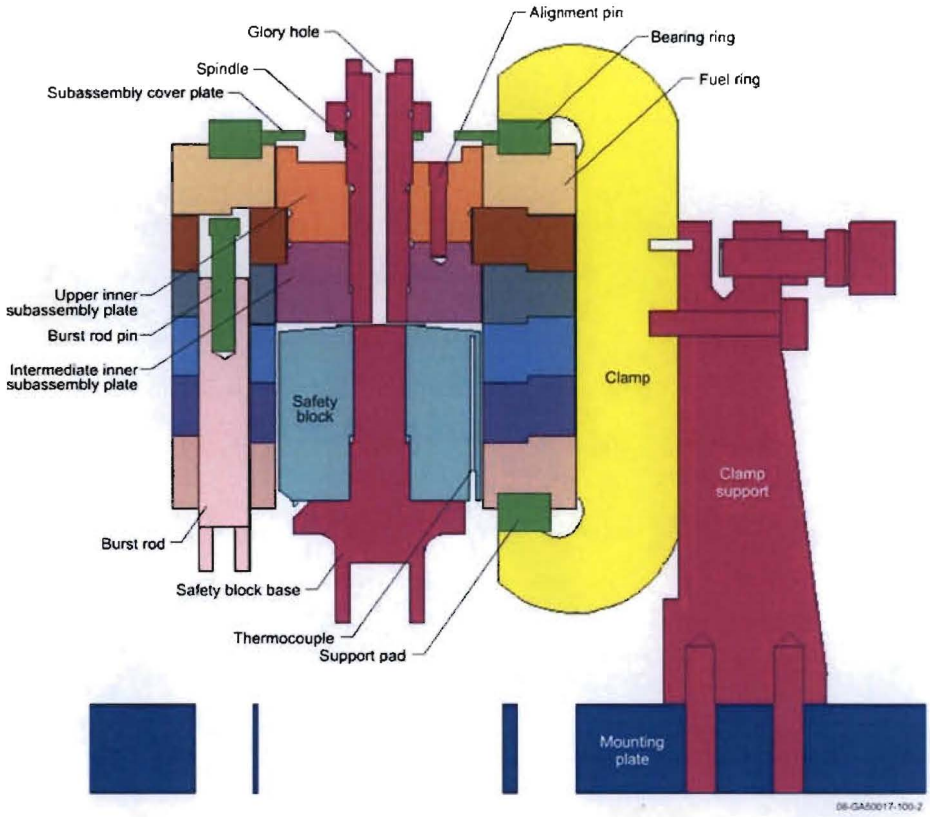

Figure 3. Schematic of the Godiva-IV core and its restraints.

was 7.544 cm, while the full strokes of control rods 1 and 2 were nominally 10.183 cm and 9.467 cm, respectively.

Table I. Control-rod and burst-rod positions

Case	Condition	Control Rod Positions (cm withdrawn)		Burst Rod Position
		Control Rod 1	Control Rod 2	
1	Delayed critical	10.163	1.140	Fully inserted
2	Delayed critical	5.075	4.232	Fully inserted
3	Delayed critical	1.252	9.637	Fully inserted
4	Delayed critical	1.191	1.135	Fully withdrawn
5	Super-prompt-critical	0.810	1.666	Fully inserted

3. DETAILED MODEL OF GODIVA-IV

A detailed model of each of the five conditions was constructed using the MCNP5 Monte Carlo code [3]. Sensitivity calculations were performed with those models to determine the experimental uncertainty associated with k_{eff}. Those calculations were performed with a combination of the ACTI [4] and ENDF66 [5] nuclear data libraries, which are included in the MCNP5 distribution. For the materials in the Godiva-IV assembly, that combination corresponds to the final version of ENDF/B-VI [6]. Each MCNP calculation employed 550 generations of 10,000 neutrons each. The first 50 generations were excluded from the statistics, thereby producing results based on 5,000,000 active neutron histories. Those same numbers of generations, histories per generation, and generations skipped also were used in all of the subsequent calculations discussed herein.

As indicated in Table II, the principal contributors to the uncertainty in k_{eff} were found to be the uncertainties in the mass of the fuel (± 0.0018 Δk), the separation between the subassembly plate and the safety block (± 0.0011 Δk), and the molybdenum content of the fuel (± 0.0009 Δk). The overall uncertainty is ± 0.0026 Δk. The measured periods for the four delayed-critical configurations were effectively infinite. Consequently, the experimental value of k_{eff} for those four cases is estimated to be 1.0000 ± 0.0026.

An additional uncertainty was estimated for the static super-prompt-critical condition based on the calculated value for β_{eff} (0.0064 ± 0.0004) and the reported initial period for the burst (30.8 μs), but it was found to be negligible relative to the overall uncertainty. The experimental value of k_{eff} for the static super-prompt-critical configuration is estimated to be 1.0066 ± 0.0026.

Subsequent MCNP5 calculations were performed for the five cases using nuclear data libraries based on ENDF/B-VII.0 [7], JEFF-3.1 [8], and JENDL-3.3 [9], in addition to ENDF/B-VI. The ENDF/B-VII.0 library is included with the current MCNP5 distribution, while the JEFF-3.1 and JENDL-3.3 libraries were obtained from the NEA Data Bank and from the Radiation Safety Information Computational Center at Oak Ridge National Laboratory, respectively. The results from those calculations are presented in Table III. All four nuclear data libraries produce consistent results: for any given library, the highest and lowest of the values of k_{eff} for the four delayed-critical cases differ by less than 0.002 Δk. In absolute terms, JENDL-3.3 clearly produces the best overall agreement with the experimental values for k_{eff}.

4. BENCHMARK AND CYLINDRICAL MODELS OF GODIVA-IV

The detailed models were transformed into simplified benchmark models by eliminating components that have little impact on reactivity (e.g., the core cover, belly band, and contamination shield), homogenizing internal voids with their surrounding regions, and simplifying the complicated geometries of several of the components. The masses of the affected fuel pieces were preserved during these transformations. Because of the similarity of the configurations, the individual changes were made only to a single case (case 2). The

Table II. Impact of experimental uncertainties on k_{eff}

Source of Uncertainty	Uncertainty in Reactivity (Δk)
Fuel mass	± 0.0018
Molybdenum content of fuel	± 0.0009
Uranium enrichment and isotopics	± 0.0003
Masses of non-fuel core components	± 0.0003
Composition of non-fuel core components	± 0.0003
Restraint masses	± 0.0004
Restraint compositions	± 0.0005
Structural support compositions	± 0.0002
Fuel dimensions	± 0.0005
Dimensions of non-nuel core components	± 0.0002
Restraint dimensions	± 0.0005
Position of safety block	± 0.0011
Positions of both control rods	± 0.0005
Period (cases 1 through 4) Period (case 5)	Negligible ± 0.0003
Cumulative (cases 1 through 5)	± 0.0026

cumulative changes then were applied to the other cases, and the results were compared to ensure that the differences between the values of k_{eff} for the detailed model and the corresponding benchmark model were consistent for all five cases. A summary of the individual changes and their impact on k_{eff} is presented in Table IV. Overall, these changes produce a negligible change in reactivity, and they reduce computation time by approximately 70%. A schematic of the benchmark model of case 2 is shown in Figure 4.

Although the results in Table II indicate a negligible bias between the values of k_{eff} for the detailed and benchmark models, the uncertainty in that bias is ± 0.0004 Δk. Direct comparisons for the individual cases produce marginally negative biases for cases 1, 2, and 3 and statistically insignificant biases for cases 4 and 5. However, there is no compelling reason to expect the bias between the benchmark and detailed models to be unique to each particular case. Consequently, an average bias for all five cases probably is more representative than a case-specific bias.

Table III. MCNP5 results for the detailed models of Godiva-IV

Case	Experimental k_{eff}	Calculated k_{eff}			
		ENDF/B-VI	ENDF/B-VII.0	JEFF-3.1	JENDL-3.3
1	1.0000 ± 0.0026	**0.9937 ± 0.0003**	**0.9966 ± 0.0003**	**0.9930 ± 0.0003**	1.0001 ± 0.0003
2	1.0000 ± 0.0026	**0.9939 ± 0.0003**	**0.9965 ± 0.0003**	**0.9930 ± 0.0003**	1.0004 ± 0.0003
3	1.0000 ± 0.0026	**0.9946 ± 0.0003**	0.9974 ± 0.0003	**0.9934 ± 0.0003**	1.0010 ± 0.0003
4	1.0000 ± 0.0026	**0.9952 ± 0.0003**	0.9983 ± 0.0003	**0.9947 ± 0.0003**	1.0017 ± 0.0003
5	1.0066 ± 0.0026	**1.0000 ± 0.0003**	**1.0036 ± 0.0003**	**0.9992 ± 0.0003**	1.0069 ± 0.0003

$\sigma < |\Delta k| \leq 2\sigma$ **$|\Delta k| > 2\sigma$**

Accordingly, the average bias of -0.0004 Δk has been applied uniformly to the experimental values for k_{eff} to produce a reference value of k_{eff} for the simplified benchmark models. The benchmark value of k_{eff} for the four delayed-critical cases therefore is 0.9996 ± 0.0026, and the benchmark value of k_{eff} for the static super-prompt-critical case is 1.0062 ± 0.0026.

Results from the four nuclear data libraries are presented in Table V for the benchmark models of all five cases. Not surprisingly, JENDL-3.3 again produces the best overall agreement with the benchmark values for k_{eff}.

The benchmark model for the static super-prompt-critical condition was further transformed into a two-dimensional cylindrical model that potentially could be the basis for calculations of the full burst with two-dimensional kinetics codes. The masses of the fuel components were preserved during this transformation, but the clamps were converted into a hollow cylinder, and the clamp supports were eliminated entirely. A vertical slice through center of the cylindrical model of the core is shown Fig. 5, and the changes in k_{eff} to convert the three-dimensional benchmark model into the two-dimensional cylindrical model are presented in Table VI.

The two dominant changes clearly are the removal of the notches in the outer edges of the fuel rings and the adjustment to produce a single outer radius for the cylinder into which the clamps have been transformed. While these two contributions largely offset each other in terms of reactivity, adjustments that produce such relatively large changes in k_{eff} would not be acceptable in the creation of a benchmark model. In this case, however, the objective is to create a two-dimensional cylindrical representation rather than a true benchmark model. When the cumulative change in k_{eff} from Table VI is applied to the benchmark value for k_{eff}, the reference value for k_{eff} for the two-dimensional cylindrical model is 1.0056 ± 0.0004.

Table IV. Impact on k_{eff} of simplifications for benchmark model

Simplification	Incremental Δk
Remove core cover	-0.0004 ± 0.0004
Remove belly band and belly-band bolts	-0.0008 ± 0.0004
Remove contamination shield	-0.0007 ± 0.0004
Convert mounting plate to flat cylinder	Negligible
Convert safety block to simple cylinder	Negligible
Convert safety block base to set of cylinders	Negligible
Convert intermediate inner subassembly plate to cylinders	Negligible
Convert upper inner subassembly plate to cylinders	0.0004 ± 0.0004
Convert spindle to hollow, uniform cylinder	-0.0006 ± 0.0004
Fill offset holes in cover plate	Negligible
Standardize notch depth for all fuel rings	Negligible
Remove thermocouple hole from fourth ring	Negligible
Fill gaps between fuel rings	-0.0007 ± 0.0004
Fill partial control/burst rod holes in fifth ring	Negligible
Remove chamfering from control rods	0.0005 ± 0.0004
Remove pin and chamfering from burst rod	Negligible
Convert support pads to ring	0.0009 ± 0.0004
Standardize bearing ring to uniform depth	0.0007 ± 0.0004
Make internal corners for clamps square	Negligible
Remove screw holes in clamps	0.0004 ± 0.0004
Make tops and bottoms of clamps flat	-0.0004 ± 0.0004
Fill holes in clamp supports	0.0004 ± 0.0004
Make clamp supports rectangular	Negligible
Cumulative	-0.0003 ± 0.0004 (Negligible)

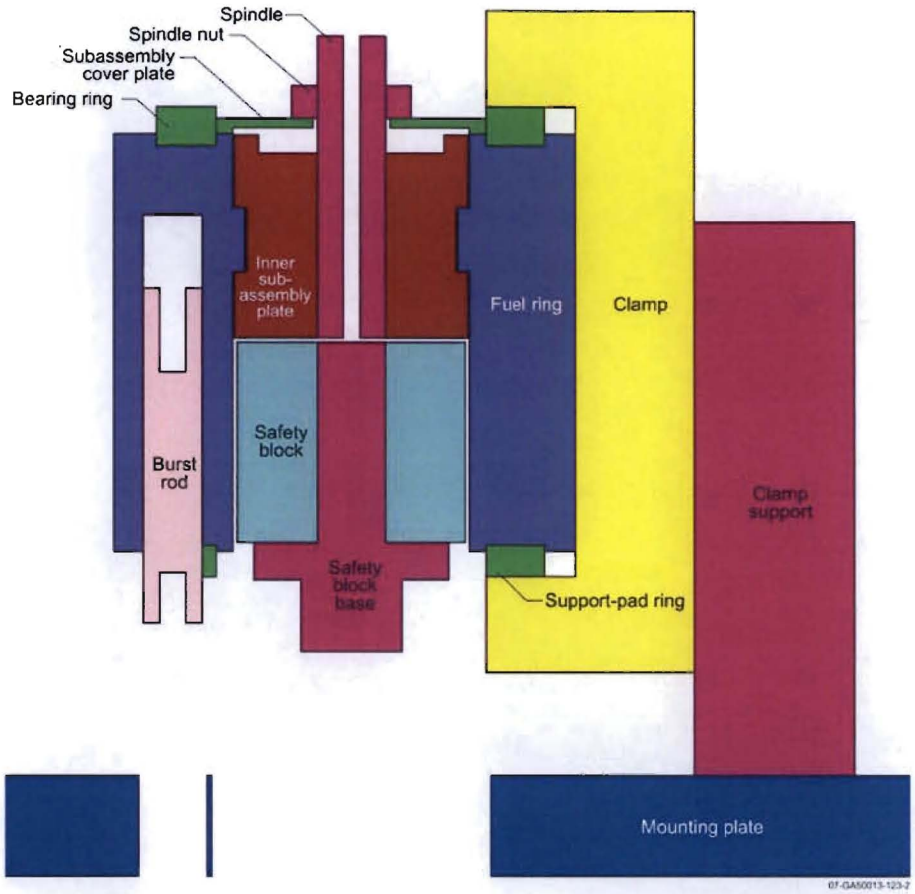

Figure 4. Vertical slice through the center of the benchmark model of Godiva-IV.

Table V. MCNP5 results for simplified benchmark models of Godiva-IV

Case	Benchmark k_{eff}	Calculated k_{eff}			
		ENDF/B-VI	ENDF/B-VII.0	JEFF-3.1	JENDL-3.3
1	0.9996 ± 0.0026	**0.9931 ± 0.0003**	**0.9960 ± 0.0003**	**0.9919 ± 0.0003**	0.9996 ± 0.0003
2	0.9996 ± 0.0026	**0.9933 ± 0.0003**	**0.9962 ± 0.0003**	**0.9924 ± 0.0003**	0.9999 ± 0.0003
3	0.9996 ± 0.0026	**0.9940 ± 0.0003**	0.9970 ± 0.0003	**0.9935 ± 0.0003**	1.0003 ± 0.0003
4	0.9996 ± 0.0026	**0.9948 ± 0.0003**	0.9979 ± 0.0003	**0.9941 ± 0.0003**	1.0015 ± 0.0003
5	1.0062 ± 0.0026	**1.0003 ± 0.0003**	**1.0028 ± 0.0003**	**0.9990 ± 0.0003**	1.0059 ± 0.0003

$\sigma < |\Delta k| \leq 2\sigma$ **$|\Delta k| > 2\sigma$**

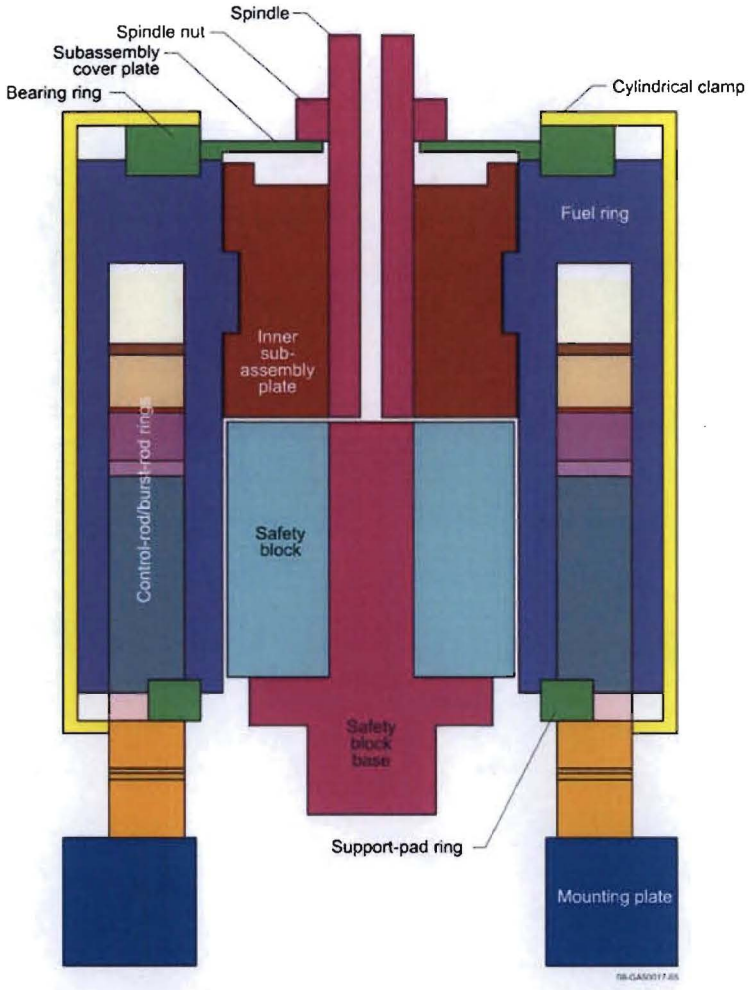

Figure 5. Vertical slice through the center of the cylindrical model of Godiva-IV.

Results from the four nuclear data libraries are presented in Table VII for the three models of the static super-prompt critical condition. JENDL-3.3 produces the best agreement with the reference values for k_{eff} for all three models.

5. SUMMARY AND CONCLUSIONS

Detailed and simplified benchmark MCNP models have been constructed for four delayed-critical experiments and for the static phase of a super-prompt-critical burst experiment performed with the Godiva-IV assembly. In addition, a two-dimensional cylindrical model has been constructed for the static super-prompt-critical condition. Complete specifications for all of those models are provided in a separate report [10].

Table VI. Impact on k_{eff} of simplifications for the cylindrical model

Modification	Δk
Remove Holes and Gaps Around Control and Safety Rods	Negligible
Convert Control Rods and Burst Rods into Rings:	-0.0001 ± 0.0004
Remove Clamp Supports	-0.0005 ± 0.0004
Remove Notches in Fuel Rings	-0.0088 ± 0.0004
Convert Top Prongs of Clamps to Cylinder	0.0008 ± 0.0004
Convert Bottom Prongs of Clamps to Cylinder	Negligible
Convert Backs of Clamps to Cylinder	0.0010 ± 0.0004
Produce Single Outer Radius for Cylindrical Clamp	0.0079 ± 0.0004
Simplify Mounting Plate	-0.0009 ± 0.0004
Cumulative	-0.0006 ± 0.0004

Table VII. MCNP5 results for the static super-prompt critical condition of Godiva-IV

Model	Reference k_{eff}	Calculated k_{eff}			
		ENDF/B-VI	ENDF/B-VII.0	JEFF-3.1	JENDL-3.3
Detailed	1.0066 ± 0.0026	**1.0000 ± 0.0003**	**1.0036 ± 0.0003**	**0.9992 ± 0.0003**	1.0069 ± 0.0003
Benchmark	1.0062 ± 0.0026	**1.0003 ± 0.0003**	**1.0028 ± 0.0003**	**0.9990 ± 0.0003**	1.0059 ± 0.0003
Cylindrical	1.0056 ± 0.0026	**0.9990 ± 0.0003**	**1.0026 ± 0.0003**	**0.9984 ± 0.0003**	1.0060 ± 0.0003

$\sigma < |\Delta k| \leq 2\sigma$ **$|\Delta k| > 2\sigma$**

The detailed models have been employed to estimate the uncertainty in k_{eff} associated with the experiments. In addition, criticality calculations have been performed for all of those models with four modern nuclear data libraries. Each library produces consistent results, with small differences among the four delayed-critical values for k_{eff}. Overall, JENDL-3.3 produces the best agreement with the experimental values for k_{eff}.

ACKNOWLEDGMENT

Figures 3, 4, and 5 were prepared by Christine White of Idaho National Laboratory.

REFERENCES

1. R. E. Peterson, "Lady Godiva: An Unreflected Uranium-235 Critical Assembly," LA-1614, Los Alamos Scientific Laboratory (1953).
2. R. J. LaBauve, "Bare, Highly Enriched Uranium Sphere (Godiva)," HEU-MET-FAST-001, *International Handbook of Evaluated Criticality Safety Benchmark Experiments*, NEA/NSC/DOC(95)03, OECD NEA Data Bank (2008 edition).
3. X-5 Monte Carlo Team, "MCNP — A General Monte Carlo Particle Transport Code, Version 5," LA-UR-03-1987, Los Alamos National Laboratory (2003).
4. S. C. Frankle, R. C. Reedy, and P. G. Young, "ACTI: An MCNP Data Library for Prompt Gamma-Ray Spectroscopy," *Proc. 12th Biennial Topl. Mtg. Radiation Protection and Shielding Div.*, Santa Fe, New Mexico, April 2002 (2002).
5. J. M. Campbell, S. C. Frankle, and R. C. Little, "ENDF66: A Continuous-Energy Neutron Data Library for MCNP4C," *Proc. 12th Biennial Topl. Mtg. Radiation Protection and Shielding Div.*, Santa Fe, New Mexico, April 2002 (2002).
6. V. McLane, Ed., "ENDF-102: Data Formats and Procedures for the Evaluated Nuclear Data File ENDF-6," BNL-NCS-44945, Brookhaven National Laboratory (Rev., 2001).
7. M. B. Chadwick, *et al.*, "ENDF/B-VII.0: Next Generation Evaluated Nuclear Data Library for Nuclear Science and Technology," *Nuclear Data Sheets*, **107**, pp. 2931-3059 (2006).
8. O. Cabellos, "Processing of the JEFF-3.1 Cross Section Library into a Continuous Energy Monte Carlo Radiation Transport and Criticality Data Library," NEA/NSC/DOC(2006)18, OECD NEA Data Bank (2006).
9. K. Shibata, *et al.*, "Japanese Evaluated Nuclear Data Library Version 3 Revision 3: JENDL-3.3," *J. Nucl. Sci. Technol.*, **39**, pp. 1125-1136 (2002).
10. R. D. Mosteller and J. M. Goda, "Godiva-IV Delayed-Critical and Static Super-Prompt-Critical Experiments," LA-UR-08-5613, Los Alamos National Laboratory (2008).